To appear in *Structural Safety*

Structural Design for Earthquake Resilience: Info-Gap Management of Uncertainty

Yoshihiro Kanno,[1] Shinnosuke Fujita[2] and Yakov Ben-Haim[3]

Contents

Abstract Resilience in recovery of critical functionality, after severe adverse events such as earthquakes, is a key concept in design of structures and infrastructures. We discuss three distinct challenges: the inherent uncertainty of the system, exogenous uncertainty of loads on the system, and vulnerability of the putative system to adverse events. We develop an info-gap robust-satisficing approach for managing these challenges. We illustrate the method with seismic examples comparing relatively flexible base-isolated structures against stiffer seismic resistant structures. These examples illustrate that the preference between these designs, based on their robustness against uncertainty, depends on the performance requirement. The potential for reversal of preference between competing designs is quantified by intersection between the info-gap robustness curves of those designs. We prove a proposition asserting conditions under which the robustness curves for two different designs will cross one another, entailing the potential for reversal of preference between the two designs. The resulting robust-satisficing design decision may differ both from performance-optimization, in which the design that is predicted to have better performance will be chosen, and from the min-max design.

Keywords: Robustness; resilience; info-gap; recovery; base-isolated structure; seismic resistent structure.

\people\kanno\resilience2016\rsl016.tex July 27, 2017

[1]Laboratory for Future Interdisciplinary Research of Science and Technology, Institute of Innovative Research, Tokyo Institute of Technology, Japan.

[2]Laboratory for Future Interdisciplinary Research of Science and Technology, Institute of Innovative Research, Tokyo Institute of Technology, Japan.

[3]Yitzhak Moda'i Chair in Technology and Economics, Faculty of Mechanical Engineering, Technion—Israel Institute of Technology, Haifa 32000 Israel. Corresponding author: yakov@technion.ac.il

1 Introduction

Resilience has become a widely-accepted key to design of structures and infrastructures against severe hazard, such as megathrust earthquakes. It is usual that structures and infrastructures are designed against the so-called assumed hazard scenarios, that are based on historical precedents and present scientific knowledge. However, like the 2011 Tohoku earthquake and tsunami, never-before-seen hazard can always happen. Mochizuki and Komendantova [31] reported that, in post-2011 Japan, it is recognized that adverse surprise, worse than historical precedents, will occur and, hence, one must plan for the unknown. Also, it is recognized that, although science is certainly useful, it always has a limit, and uncertainty, against which one must prepare plans, always remains. In this paper, we present a methodology to evaluate resilience of a structural system quantitatively, while fully addressing such severe uncertainty of future hazard.

Several definitions, or measures, of structural resilience have been proposed; see, e.g., [4] for a survey. Roughly speaking, it is commonly recognized that two key issues providing high resilience are "robustness and/or resilience to loss of functionality" and "short time to recovery"; see, e.g., [6, 10, 13, 17–19, 30, 33, 34, 42]. Among others, the so-called resilience triangle [6, 13] is often adopted to assess resilience of structures. There, functionality of a damaged structure is considered a linear function of time, and the area of the resilience triangle is defined by three points: the 100% functionality right before the damage event, the functionality right after the damage event, and the 100% functionality at the recovery time. A small value of the area of the resilience triangle is preferred over a large value. It is straightforward to generalize this definition to a nonlinear functionality function. This resilience measure has been applied to a hospital system [7, 12–15, 30], bridge and transportation networks [3, 9, 20], power networks [8], community seismic performance [10, 16], economic resilience of interdependent infrastructures [34], and braced-frame office buildings [44].

When we attempt to evaluate seismic resilience of structures, the most difficult quantity to predict is the recovery time, as pointed out in much literature [13, 21, 41]. This is because the time to recovery possesses many sources of uncertainties, including earthquake intensities, material procurement, relocation of functions, available human resources, damage in supply of daily essentials, economy, etc. Also, as mentioned above, future hazard is also difficult to predict, as we acknowledge that it can be worse than historical precedents. To assist decision-making under such severe uncertainties, this paper provides a general framework for quantifying resilience based on info-gap theory [2].

As a concrete example of resilience evaluation under uncertainty, attention in this paper is focused on seismic design of buildings. More specifically, we compare the conventional fixed-support building system, called the Seismic Resistant Structure (SRS), and the seismically base-isolated system, called the Base-Isolated Structure (BIS). We shall see that, rather surprisingly, robustness preference between these two structural designs can reverse as the resilience requirement changes.

The seismically base-isolated system has been widely used to improve seismic performance of buildings [11]. The system incorporates seismic isolators to decrease the structural response of the superstructure dramatically during a strong earthquake, compared with the conventional fixed-support buildings. On the other hand, flexibility of the seismic isolators, which is requisite for the seismically base-isolated system, results in large relative horizontal displacements of the superstructure, particularly during an earthquake excitation including long period pulses, such as near-fault ground motions [22, 29]. Therefore, sufficiently wide clearance, called the isolation gap or the seismic gap, should be left between the base of a seismically isolated building and the surrounding

moat wall. However, it is often difficult to retain sufficient width due to diverse practical restrictions, particularly in a densely built-up area. Also, earthquake loads, which are assumed in the structural design procedure to determine the width of the isolation gap, inevitably possess large uncertainties. Therefore, collision between a seismically isolated building and its surrounding moat wall may possibly be induced by strong earthquake excitation. Many studies, including experimental simulation [26], have been done on the influence of earthquake-induced pounding on seismically isolated buildings; see [23, 25, 27, 35, 36, 43, 45] and the references therein.

A seismically isolated building can also suffer earthquake-induced impact events against its adjacent conventional fixed-support buildings at the upper floor levels [1, 24, 28, 38, 39] before impact events against the surrounding moat wall. It is well known that a base-isolated building in Los Angeles actually underwent impact against its entry bridge during the 1994 Northridge earthquake [32]. Earthquake-induced pounding against either the surrounding moat wall or the adjacent fixed-support buildings can cause significant damage to the base-isolated building. This is because high vibration modes of the superstructure induced by the pounding can cause much greater acceleration response [24] and the inelastic deformation of the superstructure often concentrates at lower floors [35, 43]. Greater accelerations of floors also yield significant damage in acceleration sensitive non-structural components, such as ceilings and elevators. Although there exist some suggestions of making use of bumping or shock absorbers to mitigate the damage due to earthquake-induced pounding [23, 40, 43], it is very rare for a real-world building to incorporate such subsidiary equipment.

In short, the base-isolation system is an innovative seismic system that can reduce the inter-story drifts, shear forces, and floor accelerations of the superstructure. Therefore, one can design the superstructure of a seismically isolated building with lower stiffness compared with the conventional fixed-support building. Due to the flexibility of seismic isolators, however, a seismic isolation building may possibly undergo pounding during a large earthquake. Once pounding occurs, damage of a seismically isolated building can possibly become severer, because the superstructure has less stiffness compared with a conventional fixed-support building. Thus, an innovative and potentially better structural system has unavoidable possibilities of severer damage, from which the conventional structural system is usually free.

As a study relevant to this paper, Dong and Frangopol [21] proposed a method for evaluating the seismic sustainability and resilience of conventional and seismically isolated buildings. Given a seismic event, the probability of failure is computed to assess the seismic performance of structural and nonstructural components. Then the probability distribution of the recovery time is assumed in order to evaluate the resilience of a building. They conclude that the base-isolation system can drastically reduce the seismic repair loss, down-time, and fatalities, compared with the conventional fixed-support building system. The approach presented in this paper does not need to specify the seismic event. Rather, the intensity, earthquake center, dominant period of earthquake excitation, and other properties of the seismic event are considered uncertain. Also, our approach is applicable even if reliable stochastic information of the recovery time is not available.

To develop reliable methods for evaluating the seismic resilience of structures, one may attempt to construct sophisticated models of the recovery time and the loss of functionality of structures by integrating diverse details reflecting the reality. Much effort has been done, as found in the literature cited above. However, no matter how much the models are elaborated, it is not possible to predict the structural resilience precisely, due to the uncertainty and the limitation of science mentioned above. In this paper, we focus on this fact, and present a general framework, based on the info-gap theory,

for decision-making under uncertainty. The two most distinctive features of info-gap theory are (i) it does not depend on knowledge of probability distributions, and (ii) it does not presume knowledge of a worst case. Any method for evaluating the structural resilience can be incorporated into this framework, and the structural designs under consideration will be ranked in terms of robustness against uncertainty for satisfying the requirement on the structural resilience. Info-gap theory [2] is a suitable, and implementable, methodology for developing such a framework.

The paper is organized as follows. Section 2 presents a conceptual discussion of vulnerability, uncertainty and robustness, along with simple examples of the proposed method for quantifying resilient performance under uncertainties. Section 3 presents a numerical example to explore the modelling and management of both inherent and exogenous uncertainty in a realistic setting. Section 4 establishes a proposition that provides a sufficient condition for existence of preference reversal between two structural systems such as SRS and BIS. Some conclusions are drawn in section 5.

2 Preliminary Examples: Vulnerability, Uncertainty and Robustness

2.1 Conceptual Discussion

In this section we discuss the distinctions between inherent vulnerability of a structure, inherent uncertainty of a structure, and vulnerability to exogenous uncertainty. We demonstrate how prioritization of design options is based on the info-gap approach to robustness to uncertainty in response to all three of these challenges. The discussion is illustrated with two simple examples. Section 3 contains a more realistic example.

In order to provide clarity to the generic discussion, consider two different design concepts for a structure for seismic safety: Seismic Resistant Structure (SRS) and Base-Isolated Structure (BIS). It is important to note that the method presented in this paper is applicable to any structural systems. Roughly speaking, an SRS is designed to be very stiff. The stiffness of the structure prevents major damage over a large range of seismic loading, but the stiffness also results in damage even at low loads, increasing in severity as the load increases. In contrast, a BIS structure is built on flexible bearings or pads that isolate the structure from the earthquake motion, but allow larger motion of the entire structure. Damage begins to accumulate in a BIS only at higher seismic loads than in an SRS. However, large displacements can result in a BIS at large loads, resulting in closure of clearance to surrounding obstructions and more severe damage than an SRS at large load. In rough summary, a BIS is safer at low or moderate loads while a BIS can be less safe than an SRS at larger loads.

Both BIS and SRS have **inherent vulnerability:** the potential for large and damaging displacements. Any vulnerability that is a pre-existing state of the system is called inherent vulnerability. [5, 46]. This vulnerability is greater for a BIS than for an SRS at large loads, but the situation is reversed at low loads. The vulnerability is an inherent attribute of the dynamic model of the structure, and is not a result of structural uncertainty or of uncertainty in the load.

Both BIS and SRS have **inherent uncertainty** in their performance. Material properties, physical dimensions, and static and dynamic properties are estimated and modeled, some with greater accuracy and precision than others. This type of uncertainty derives from the structure itself and its subsystems, and is called inherent uncertainty (also referred as endogenous uncertainty [37]). Resilience of functional characteristics depends on many factors inherent to the system, including its support network, that are imperfectly or even poorly known. Consequently, seismic damage to the structure may be worse (or better) than anticipated from a design-base load simply due to deviation

of the actual structure or its operational environment from its conceptualization by the designer. The inherent uncertainty of a structure means that its inherent vulnerabilities may be greater or less than anticipated.

Both a BIS and an SRS are vulnerable to **exogenous uncertainty** in the amplitude and temporal waveform of the seismic load. Either structure could be designed to perform adequately for specified load levels, but surprisingly large loads can result in failure. This type of uncertainty is sourced from the environment, and is called the exogenous uncertainty [37]. This exogenous uncertainty in the load is not an inherent vulnerability nor an inherent uncertainty of the structure, though exogenous uncertainties can exacerbate an inherent vulnerability.

The design methodology for managing all three challenges—inherent vulnerability, inherent uncertainty, and exogenous uncertainty—is based on the idea of **robustly satisfying** critical performance requirements [2]. The designer identifies the critical functional attributes that must be achieved in order for the structural performance to be adequate. For example, following an earthquake, basic structural integrity must never be lost and electric power must be recovered within a specified duration after the event. The designer will prioritize the design alternatives in terms of their robustness-against-uncertainty for satisfying the critical performance requirements. A system is highly robust if the performance is adequate for any realization over a large range of surprise. A system has low robustness if even small deviations can result in unacceptable performance. A highly robust design is preferred over a design with low robustness. This is called “robust satisficing”, where “to satisfice” means “to satisfy critical performance requirements”.

Note that robust satisficing is different from prioritizing design alternatives in terms of their predicted performance. A design methodology that could be called “performance optimization” would rank design alternatives in terms of the substantive quality of their predicted performance. For instance, a structure whose predicted amplitude of displacement in response to an earthquake is low, would be preferred over a structure with larger predicted displacement. The robust satisficing methodology ranks the alternatives in terms of their robustness against uncertainty for satisfying performance requirements, and not in terms of their predicted performance. The robust-satisficer will optimize the robustness, while the performance-optimizer will optimize the predicted behavior of the structure. These two strategies may, or may not, lead to the same design decision, and in any case will entail different design considerations, as we now illustrate with two simple examples. A more detailed example is developed in section 3.

2.2 Time to Recovery with Inherent Vulnerability and Exogenous Uncertainty

An important property of many technological systems is the time to recovery (TTR) after a disruptive event. A building after an earthquake, an airplane after loss of an engine, urban infrastructure after a flood, etc., all need to recover critical functionalities within specified times. We will illustrate the concepts of inherent vulnerability and exogenous uncertainty, and the methodology of info-gap robust satisficing, by comparing the two seismic design concepts discussed earlier: SRS and BIS. We will illustrate the concept of inherent uncertainty in section 2.3.

We first briefly summarize the analysis of robustness in info-gap theory [2], which is based on the following three elements:

- The system model that describes the behavior of the system. In our case, we focus on models of SRS and BIS.

- The performance requirement that specifies functionalities that the system must achieve. The performance requirement that we consider is the structural resilience evaluated in terms of TTR.

- The uncertainty model called the info-gap model. This is an unbounded family of nested sets of possible realizations of uncertain parameters or functions.

Suppose that a system performance of interest is given as a function of a system parameter x. We use $g(x)$ to denote the system performance, where we assume that a small value of $g(x)$ is preferred over a large value. Consider the performance requirement

$$g(x) \leq g_{\rm c} \tag{1}$$

where $g_{\rm c}$ is the maximal allowable value. Suppose that x has uncertainty. Let $\tilde{x}$ denote the nominal value (or the best estimate) of x. We use $\mathcal{X}(\alpha, \tilde{x})$ to denote the set of possible realizations of x , where $\alpha \geq 0$ is a parameter representing the level of uncertainty, called the horizon of uncertainty. An info-gap uncertainty model has two properties: (i) $\mathcal{X}(0, \tilde{x}) = \{\tilde{x}\}$ (called contraction), and (ii) $\alpha > \alpha' \geq 0$ implies $\mathcal{X}(\alpha, \tilde{x}) \supseteq \mathcal{X}(\alpha', \tilde{x})$ (called nesting). That is, (i) $\alpha = 0$ means the absence of uncertainty, and (ii) the range of possible realizations of x increases as α increases. The robustness function is defined as the maximal value of the horizon of uncertainty up to which the performance requirement is satisfied:

$$\hat{\alpha}(\tilde{x}, g_{\rm c}) = \max\Big\{\alpha : \Big(\max_{x \in \mathcal{X}(\alpha, \tilde{x})} g(x)\Big) \leq g_{\rm c}\Big\}.$$

By definition, any element of $\mathcal{X}(\hat{\alpha}(\tilde{x}, g_{\rm c}), \tilde{x})$ satisfies the performance requirement, eq.(1). Therefore, if follows from the nesting property of the info-gap model that a larger value of the robustness function means immunity to a larger horizon of uncertainty.

We are now in position to apply the info-gap theory to the robustness analysis of an SRS and a BIS. We require that the TTR of basic functions of the structure, after an earthquake event, not exceed a critical value, $t_{\rm c}$. Let $t_q(a)$ denote the TTR after a seismic event whose load amplitude is a, where $q = 0$ denotes SRS and $q = 1$ denotes BIS.

The TTR functions for the two designs, SRS and BIS, are:

$$t_0(a) = \begin{cases} 0, & \text{if } a < \beta_0 \\ \alpha_0(a - \beta_0), & \text{if } a \geq \beta_0 \end{cases} \tag{2}$$

$$t_1(a) = \begin{cases} 0, & \text{if } a < \beta_1 \\ \alpha_1(a - \beta_1), & \text{if } \beta_1 \leq a < \delta_1 \\ \gamma_1(a - \delta_1) + \alpha_1(\delta_1 - \beta_1), & \text{if } \delta_1 \leq a \end{cases} \tag{3}$$

where:

$$\gamma_1 > \alpha_q > 0, \quad \delta_1 > \beta_1 > \beta_0 > 0 \tag{4}$$

The left hand inequality of eq.(4) is intended to state that γ_1 exceeds both α_0 and α_1, both of which are positive.

These TTR functions are illustrated in fig. 1.[1] The recovery times for both design concepts increase as the earthquake load increases. The SRS ($q = 0$) has greater TTR than the BIS ($q = 1$) at low and intermediate loads, while BIS recovers more slowly at large loads.

[1] In sections 2.2 and 2.3, we present the fundamental methodology of the proposed method by using simple examples. For simple presentation, the units are omitted. Alternatively, the reader may regard variables as dimensionless quantities.

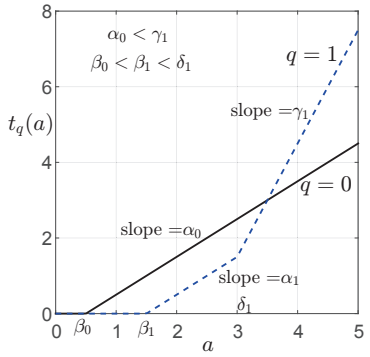

Figure 1: Recovery-time functions for example in section 2.2. $\alpha_0 = \alpha_1 = 1$, $\gamma_1 = 3$, $\beta_0 = 0.5$, $\beta_1 = 1.5$, $\delta_1 = 3$.

The performance requirement for either structure, in this simplified example, is that the TTR not exceed the critical value t_c:

$$t_q(a) \le t_c \tag{5}$$

Both structures have inherent vulnerabilities with respect to this performance requirement: there is some load level (different for each design) at which the TTR function for that design, either eq.(2) or (3), would violate the performance requirement in eq.(5).

In this simple example we will suppose that the load amplitude is estimated to be $\widetilde{a}$, and that the true amplitude, a, could deviate by as much as $\pm s$ or more where s is a known positive error estimate. We have no probabilistic information about the load. While the load amplitude must by definition be positive, we do not know the fractional error of the true amplitude, a, with respect to the estimate, $\widetilde{a}$. This exogenous uncertainty is represented by the following fractional-error info-gap model:

$$\mathcal{U}(h) = \left\{ a : \ a \ge 0, \ \left| \frac{a - \widetilde{a}}{s} \right| \le h \right\}, \quad h \ge 0 \tag{6}$$

$\mathcal{U}(h)$ is the set of all non-negative load amplitudes whose fractional deviation from the estimate is no greater than h. $\mathcal{U}(h)$ is a set-valued function of the parameter h. That is, the info-gap model is the unbounded family of nested sets, $\mathcal{U}(h)$, of load amplitudes. There are two levels of uncertainty here. For given h, the value of a is unknown within an interval, but also the value of h is unknown. The uncertainty sets $\mathcal{U}(h)$ become more inclusive as h increases, which endows h with its meaning as an 'horizon of uncertainty'. There is no known worst case because the horizon of uncertainty is unknown, as expressed by the assertion '$h \ge 0$' in eq.(6).

The info-gap method of robust satisficing combines three components: the system model $t_q(a)$ in eqs.(2) or (3), the performance requirement t_c in eq.(5), and the uncertainty model $\mathcal{U}(h)$ in eq.(6). The robustness is the greatest horizon of uncertainty, h, up to which the system model $t_q(a)$ satisfies the performance requirement for all realizations of the uncertain load a. The formal definition of the robustness function is:

$$\widehat{h}_q(t_c) = \max \left\{ h : \ \left(\max_{a \in \mathcal{U}(h)} \ t_q(a) \right) \le t_c \right\} \tag{7}$$

$\widehat{h}_q(t_c)$ is the robustness of design q for requirement t_c, which is the greatest horizon of uncertainty h up to which $t_q(a)$ does not exceed t_c for all loads a in $\mathcal{U}(h)$.

The evaluation of the robustness function is discussed in appendix A. Robustness curves are plotted in fig. 2.

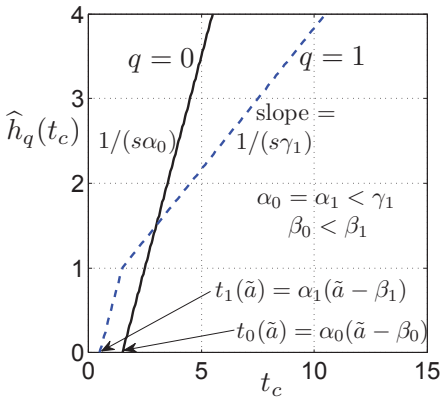

Figure 2: Robustness functions for example in section 2.2. Same parameters as fig. 1. $\widetilde{a} = 2$, $s = \widetilde{a}/2$.

The labels on the robustness curves in fig. 2 demonstrate that the curves will cross each other for any choice of parameter values obeying the specified constraints on the coefficients. This crossing of the robustness curves implies the potential for a reversal of preference between the designs, which bears directly on the distinction between robust satisficing and outcome-optimizing, as discussed at the end of section 2.1: The design that is predicted to be best is not necessarily the most robust against uncertainty for satisfying a specified requirement.

The crossing of the robustness curves in fig. 2 results from the greater **vulnerability** of BIS (due to the finite isolation gap size), and not from greater **uncertainty** in the performance of the BIS design. We see this in fig. 1, where the recovery-time curves cross even for the nominal, design-base values of the coefficients. That is, BIS is predicted to be worse than SRS at large load, **not** due to uncertainty, but due to the inherent vulnerability of BIS.

Nonetheless, the crossing of the robustness curves in fig. 2 does result from uncertainty, namely, from exogenous uncertainty in the load. Let $a_\times$ denote the load level in fig. 1 at which the putative TTR curves cross. If we knew that the true load were less than $a_\times$, then we would know that BIS would have lower recovery time than SRS. BIS recovers more quickly than SRS if the true load is less than $a_\times$, and BIS recovers more slowly otherwise.

This implies that the robustness of BIS to load-uncertainty is either greater, or less, than the robustness of SRS, depending on the critical recovery time, t_c. Uncertainty in the load (not uncertainty in BIS) can, at large enough load-deviation, exploit the greater vulnerability of BIS at large load. The properties of the BIS design are not more uncertain than properties of the SRS (in this example). However, BIS has greater vulnerability than SRS that can be activated at unexpectedly large load.

The intersection between the robustness curves in fig. 2 entails a reversal of preference between the two design options, and demonstrates the difference between robust satisficing and outcome-optimizing, as we now explain.

The outcome-optimizer will use the best available models to estimate the TTR's for each design at the best estimate of the load, which we denote $t_q(\widetilde{a})$. The outcome-optimizer will choose the design for which this TTR estimate is lowest. Design q is preferred over design q' by the outcome-optimizer if:

$$t_q(\widetilde{a}) < t_{q'}(\widetilde{a}) \tag{8}$$

The robust satisficer will choose the design with greater robustness against uncertainty, for satisfying the performance requirement. Design q is preferred over design q' by the robust-satisficer if:

$$\widehat{h}_q(t_c) > \widehat{h}_{q'}(t_c) \tag{9}$$

These designers are optimizing different functions: one optimizes the predicted outcome, the other optimizes the robustness against uncertainty for attaining acceptable outcome.

Let $t_\times$ denote the value on the t_c axis of fig. 2 at which the robustness curves cross one another. The two design methods will agree on the design (but for different reasons) if and only if $t_c < t_\times$.

We can also understand that the robust satisficing method is different from what is often called "min-max", namely, minimizing the worst anticipated outcome. Let $h_\times$ denote the value on the vertical robustness axis of fig. 2 corresponding to $t_\times$. The min-maxer starts by identifying a worst case. In the present context that can be understood as choosing the greatest horizon of uncertainty of the load, call this $h_{\max}$. The min-maxer will choose the design whose worst outcome at uncertainty $h_{\max}$ is lowest. As explained in appendix A, the horizontal axis of fig. 2 is the greatest TTR for the corresponding horizon of uncertainty on the vertical axis. We see from fig. 2 that the min-maxer will choose BIS ($q = 1$) if the greatest horizon of uncertainty is less than $h_\times$, because for this range of uncertainty BIS has lower TTR. The min-maxer will choose SRS otherwise.

The robust satisficer, as we have explained, will choose the design whose robustness for requirement t_c is greatest. The robust satisficer and the min-maxer may either agree or disagree on the design. For example, suppose the min-maxer assumes that the horizon of uncertainty cannot be greater than 3 in fig. 2. The min-max design is SRS ($q = 0$) whose worst-case TTR is less than for BIS at this horizon of uncertainty. Suppose the critical TTR for the robust satisficer is $t_c = 2$. Then, even if the robust satisficer agrees that the uncertainty could be as large as 3, or even more, the robust satisficer will disagree with the min-maxer and will prefer BIS ($q = 1$) because it is more robust at this performance requirement. But if the robust satisficer views a larger t_c as acceptable, in fact, any value greater than $t_\times$, then the robust satisficer will prefer SRS ($q = 0$) and thus agree with the min-max, though for different reasons.

2.3 Time to Recovery with Inherent Uncertainty

We now consider a simple example of robustness analysis for selecting between two designs, given inherent uncertainty in those designs. One design is the State of the Art (SotA) and the other is New and Innovative (NaI). (One could consider the distinction between SotA and NaI as a generalization of the distinction between SRS and BIS, respectively.) The SotA design is the current best practice, while the NaI purports to provide even better performance. While NaI is responsibly considered a legitimate design option, it nonetheless is accompanied with greater inherent uncertainty because of its newness: less experience has accumulated with NaI than with SotA. We are considering the inherent uncertainty in these design alternatives.

Let the system model continue to be Time to Recovery (TTR) after an adverse event of severity a, with the following estimated TTR functions for the two designs, where SotA is denoted by $q = 0$ and NaI by $q = 1$:

$$\widetilde{t}_q(a) = \begin{cases} 0 & \text{if } a < \beta_q \\ \alpha(a - \beta_q)^2 & \text{else} \end{cases} \tag{10}$$

Assume that $\beta_1 > \beta_0 > 0$ and $\alpha > 0$. Note that the estimated TTR for the SotA ($q = 0$) is longer than for the NaI for all loads greater than β_0.

The event severity is not uncertain and is known to equal $\widetilde{a}$, where $\widetilde{a} > \beta_1$. However, the true recovery-time functions, $t_q(a)$, are fractionally uncertain, so the info-gap model of inherent uncertainty of each system is:

$$\mathcal{U}_q(h) = \left\{ t_q(a): \;\; t_q(a) \geq 0, \;\; \left| t_q(a) - \widetilde{t}_q(a) \right| \leq h w_q \widetilde{t}_q(a) \right\}, \;\; h \geq 0, \;\; q = 0, 1 \tag{11}$$

This info-gap model is an unbounded family of nested sets of TTR functions for design q, $t_q(a)$ for all values of a, and reflects the uncertain shape of these functions. Each w_q is known and positive and $w_1 \widetilde{t}_1(\widetilde{a}) > w_0 \widetilde{t}_0(\widetilde{a})$ to reflect the greater uncertainty of the NaI design.

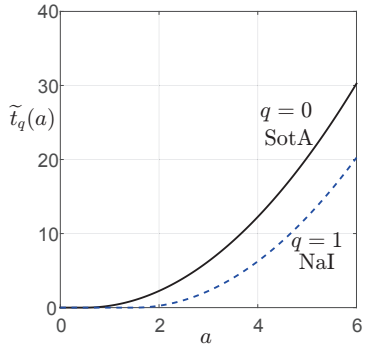

Figure 3: Recovery-time functions for the example in section 2.3. $\alpha = 1$, $\beta_0 = 0.5$, $\beta_1 = 1.5$.

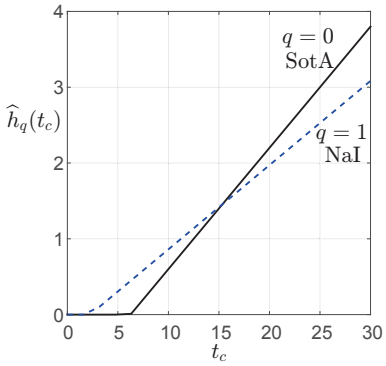

Figure 4: Robustness functions for the example in section 2.3. Same parameters as fig. 3. $\widetilde{a} = 3$, $w_0 = 1$, $w_1 = 4$.

The estimated TTR functions of eq.(10) are plotted in fig. 3 for particular choices of the coefficients, illustrating that the NaI is predicted to be less vulnerable to adverse events than the SotA design, which will be true for any coefficients obeying the specified constraints.

As in the example of section 2.2, we require that the actual TTR not exceed the critical value t_c, eq.(5). The robustness of design q is the greatest horizon of uncertainty up to which uncertainty in the shape of the TTR function does not jeopardize the achievement of the performance requirement. The robustness is defined formally as:

$$\widehat{h}_q(t_c) = \max \left\{ h: \;\; \left(\max_{t_q(a) \in \mathcal{U}_q(h)} t_q(a) \right) \leq t_c \right\} \tag{12}$$

which is readily shown to equal:

$$\widehat{h}_q(t_c) = \frac{1}{w_q} \left(\frac{t_c}{\widetilde{t}_q(\widetilde{a})} - 1 \right) \tag{13}$$

or zero for t_c values for which this is negative. Robustness curves for the two designs are plotted in fig. 4. These curves cross one another, illustrating the potential for reversal of preference between the design options, as explained in connection with fig. 2. Specifically, the performance-optimizer and the robust-satisficer may either agree, or disagree, depending on the maximum acceptable TTR.

3 Example: Inherent and Exogenous Uncertainty

In this section we present a numerical example that compares robustness of seismic resilience properties of an SRS ($q = 0$) and a BIS ($q = 1$), under both inherent and exogenous uncertainties.

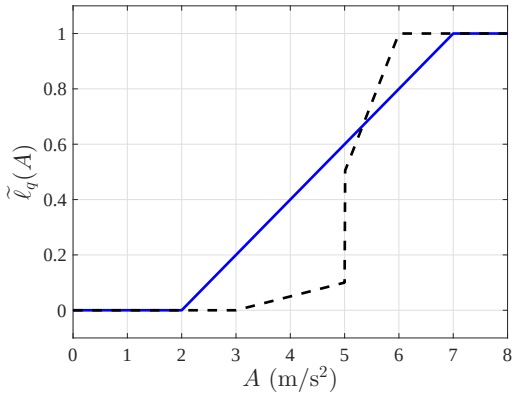

Figure 5: Loss-of-functionality functions. SRS (solid); BIS (dashed).

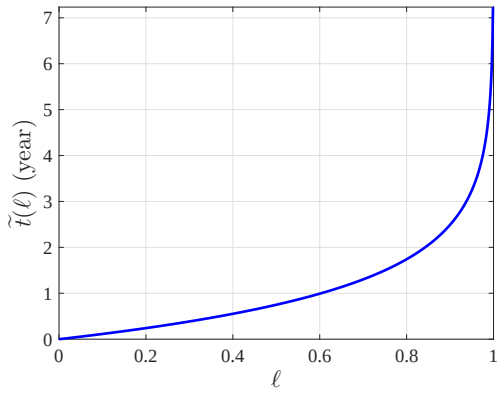

Figure 6: Time to recovery as a function of the loss of functionality.

We use simple models that roughly describe the loss of functionality and the time to recovery of these two structures. Various numerical approaches have been proposed to predict the loss of functionality and the time to recovery; see, e.g., [13, 21, 41, 44]. Any approach can be adopted in the framework presented below. The purpose of the present analysis is not to explore the properties of a specific dynamic model, but to explore the modelling and management of uncertainty in any model that one might use. It should also be clear that we use an SRS and a BIS just to illustrate the application and the implication of the proposed method. The proposed method is generic, and hence can be used to compare the resilience performance of any structures, as far as a method for predicting a recovery-time function is available. For instance we can compare two different BIS designs. Also, structural systems other than SRS and BIS can be considered.

The robustness analysis can be performed in the same manner as sections ttr in vul ex unc and ttr inh unc, although in this section we address exogenous and inherent uncertainties simultaneously. The procedure of the analysis is summarized as follows.

1. Prepare the recovery-time functions of the structures under consideration. Any existing methods can be adopted for this purpose. In the following, we assume that the time to recovery is obtained as a function of the loss of functionality, and the loss of functionality is obtained as a function of the response acceleration. Therefore, the time to recovery can be represented as a function of the response acceleration.

2. Construct the info-gap model(s) of uncertain parameter(s) and/or uncertain function(s). In this section, we assume that the response acceleration, the loss-of-functionality function, and the time-to-recovery function are uncertain, and construct their info-gap models.

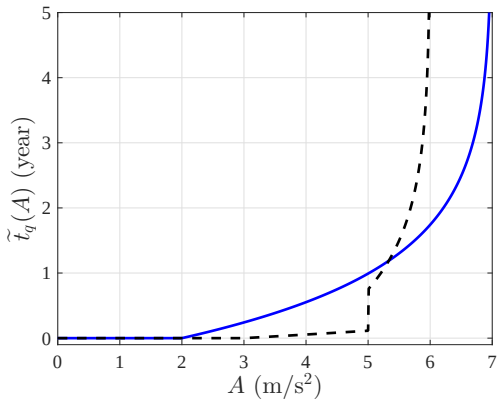

Figure 7: Estimated time to recovery as a function of the seismic load amplitude. SRS (solid); BIS (dashed).

3. Compute the robustness function to see its variation with respect to the critical recovery time.

4. Compare the obtained curves of the two structures to interpret the robustness preference.

Consider two designs, an SRS and a BIS. Let A denote the response acceleration of a structure subjected to seismic loading. We use $\ell_q(A)$ to denote the loss of functionality due to the seismic damage, for $q = 0, 1$, where $\ell_q(A) \in [0, 1]$ $(\forall A \geq 0)$ as shown in fig. 5. The value $\ell_q(A) = 0$ means that the structure suffers no damage, while $\ell_q(A) = 1$ means functionality of the structure is completely lost. We assume that $\ell_q(A)$ is a monotonically increasing function. Several numerical approaches, e.g., a scenario-based performance assessment [21], are available to estimate $\ell_q(A)$. The numerical results obtained by any approach can be adopted, as long as $\ell_q(A)$ is monotonically increasing with respect to A.

As mentioned in section 2.1, an SRS suffers damage even at low loads, compared with a BIS. In contrast, almost no damage is accumulated in a BIS, as long as the base-isolation system works properly. At large load, a BIS undergoes pounding, which causes severe damage. In fig. 5, we assume that damage of the BIS increases discontinuously at the minimum response acceleration level that induces pounding. The slope of the loss of functionality after this level is larger than that of the SRS, because the superstructure of a BIS is less stiff than an SRS.

Let $\widetilde{A}$ denote the estimate of the response acceleration. Since the seismic loading has uncertainty, the true response acceleration can deviate from $\widetilde{A}$. In a manner similar to eq.(6), this uncertainty is represented by the following info-gap model:

$$\mathcal{A}(h) = \left\{ A : A \geq 0, \ \left| \frac{A - \widetilde{A}}{w_A} \right| \leq h \right\} \tag{14}$$

Here, $w_A > 0$ is a constant. The loss of functionality cannot be predicted only from A, because it could depend on many factors, including the dominant period and duration of earthquake excitation, unknown seismic properties of nonstructural components, etc. Therefore, for given A, the shape of the function $\ell_q(A)$ has uncertainty. In a manner similar to eq.(11), this functional uncertainty is represented by the following info-gap model:

$$\mathcal{L}_q(h) = \left\{ \ell_q(A) : \ 0 \leq \ell_q(A) \leq 1, \ \left| \frac{\ell_q(A) - \widetilde{\ell}_q(A)}{w_{\ell,q}} \right| \leq h\widetilde{\ell}_q(A) \right\}, \quad q = 0, 1 \tag{15}$$

where $\widetilde{\ell}_q(A)$ is the estimate of $\ell_q(A)$, and $w_{\ell,0}$ and $w_{\ell,1}$ are positive constants.

For a given loss of functionality, ℓ, let $t(\ell)$ denote the time to recovery. We assume that t is a monotonically increasing function. Also, we assume $t(0) = 0$, i.e., no damage means zero recovery time, and $t(1) = \infty$, i.e., complete loss of functionality means incapability of recovery. An example of t is shown in fig. 6. Any function satisfying the assumptions above, that might be obtained from a numerical approach to assess the time to recovery, can be adopted in our framework. Here, we assume a simple form for the estimated TTR function:

$$\widetilde{t}(\ell) = -\kappa \ln(1 - \ell) \tag{16}$$

where $\kappa > 0$ is a constant. As mentioned in the literature [13, 21, 41], it is very difficult to predict the time to recovery. In other words, even if the loss of functionality $\ell_q(A)$ were known, the shape of the function $t(\ell_q(A))$ still possesses large uncertainty. This uncertainty is represented by:

$$\mathcal{T}(h) = \left\{ t(\ell) : t(\ell) \geq 0, \ \left| \frac{t(\ell) - \widetilde{t}(\ell)}{w_t} \right| \leq h\widetilde{t}(\ell) \right\} \tag{17}$$

where $\widetilde{t}(\ell)$ is the estimated function and $w_t > 0$ is a constant. For a given response acceleration, A, the estimated time to recovery for the two designs are given as $\widetilde{t}(\ell_q(A))$ $(q = 0, 1)$, as shown in fig. 7.

The robustness function is defined formally as:

$$\widehat{h}_q(t_\mathrm{c}) = \max \left\{ h : \left(\max_{\substack{t(\ell_q(A)) \in \mathcal{T}(h) \\ \ell_q(A) \in \mathcal{L}_q(h) \\ A \in \mathcal{A}(h)}} t(\ell_q(A)) \right) \leq t_\mathrm{c} \right\} \tag{18}$$

For given $h \geq 0$, define $A^\star(h)$, $\ell_q^\star(h)$, and $t_q^\star(h)$ by:

$$A^\star(h) := \max\{A : A \in \mathcal{A}(h)\} \tag{19}$$

$$\ell_q^\star(h) := \max\{\ell_q(A) : \ell_q(A) \in \mathcal{L}_q(h), \ A \in \mathcal{A}(h)\} \tag{20}$$

$$t_q^\star(h) := \max\{t(\ell_q(A)) : t(\ell_q) \in \mathcal{T}(h), \ \ell_q(A) \in \mathcal{L}_q(h), \ A \in \mathcal{A}(h)\} \tag{21}$$

It follows from the definitions of the info-gap models $\mathcal{A}$, $\mathcal{L}_q$, and $\mathcal{T}$ (in eqs.(14), (15), and (17)) and the monotonicity of $\widetilde{\ell}_q(A)$ and $\widetilde{t}(\ell)$ that the inner maximization in eq.(18) can be solved as:

$$A^\star(h) = \widetilde{A} + w_A h \tag{22}$$

$$\ell_q^\star(h) = \min\{1, (1 + w_{\ell,q} h)\widetilde{\ell}_q(A^\star(h))\} \tag{23}$$

$$t_q^\star(h) = (1 + w_t h)\widetilde{t}(\ell_q^\star(h)) \tag{24}$$

By using eqs.(22)–(24), we can compute $\widehat{h}_q(t_\mathrm{c})$ in eq.(18) in a manner similar to section 2.3.

For numerical examples we set $\widetilde{A} = 4\,\mathrm{m/s^2}$ and $w_A = 0.1\widetilde{A}$ in eq.(14), and κ in eq.(16) is chosen so that $t(1/2) = 3/4\,\mathrm{year}$. As for the values of $(w_{\ell,0}, w_{\ell,1}, w_t)$, we consider three cases: $(w_{\ell,0}, w_{\ell,1}, w_t) = (0.02, 0.02, 0.05)$, $(0.02, 0.02, 0.5)$, and $(0.01, 0.05, 0.05)$, representing different levels of relative uncertainty of $\ell_0(A)$, $\ell_1(A)$ and $t(\ell)$.

Robustness curves for the two designs are shown in fig. 8. In each case, the two curves cross one another. Fig. 8(b) represents much larger uncertainty in the estimate of time to recovery, $t(\ell)$, than fig. 8(a). As a result, the value of t_c at which the two curves cross, denoted $t_\times$, is larger in 8(b) than in 8(a). Consequently, the BIS (dashed) is preferable to the SRS (solid) over a broader range

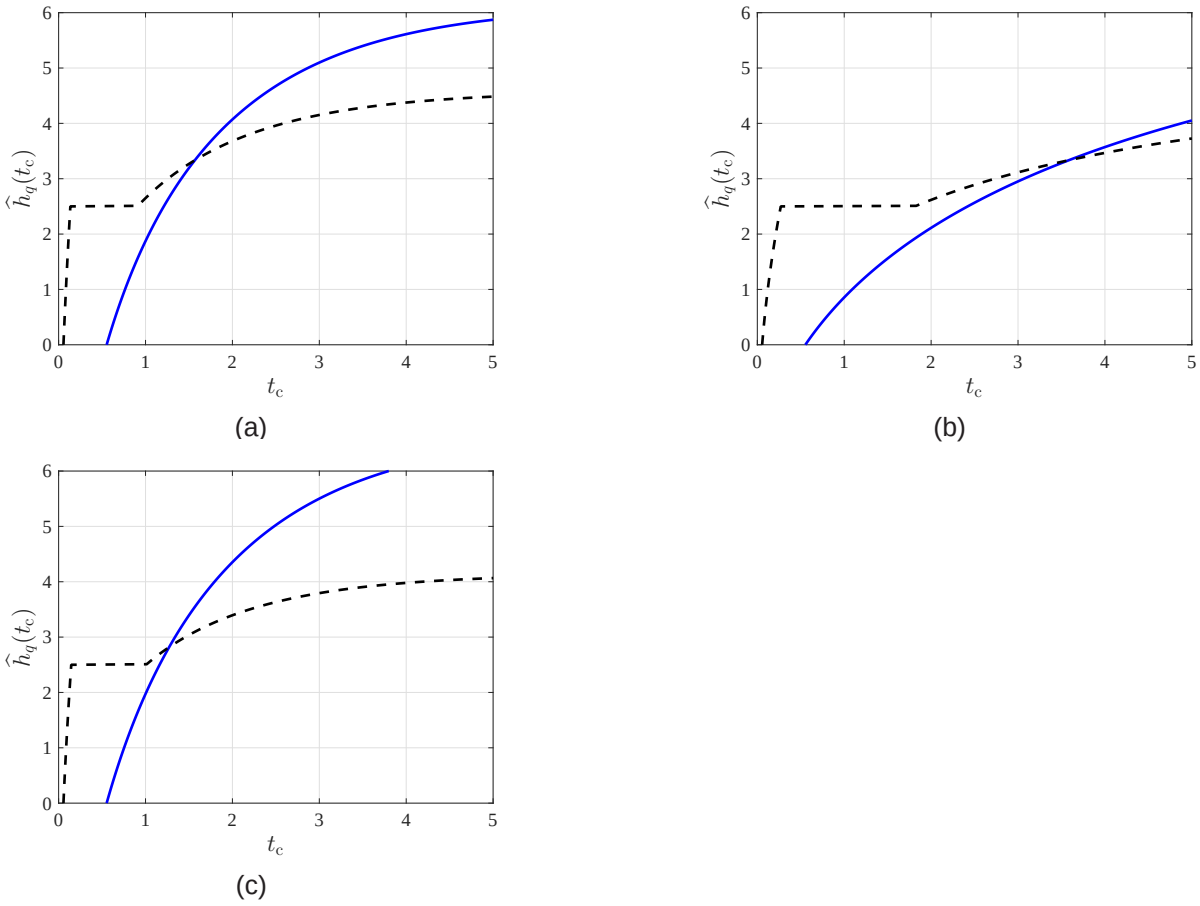

Figure 8: Robustness functions for the example in section 3. SRS (solid); BIS (dashed). (a) $(w_{\ell,0}, w_{\ell,1}, w_t) = (0.02, 0.02, 0.05)$; (b) $(w_{\ell,0}, w_{\ell,1}, w_t) = (0.02, 0.02, 0.5)$; (c) $(w_{\ell,0}, w_{\ell,1}, w_t) = (0.01, 0.05, 0.05)$.

of the critical values for the time to recovery in fig. 8(b) than in fig. 8(a). In other words, the SRS is preferable to the BIS only when a large time span is allowed for recovery, fig. 8(b). In fig. 8(a), reversal of the preference between SRS and BIS occurs at a smaller value of the time span than in fig. 8(b).

In fig. 8(c) the uncertainty weights $w_{\ell,0}$ and $w_{\ell,1}$ reflect the relatively greater uncertainty of $\ell_1(A)$ for the BIS (a rather innovative system), as compared against $\ell_0(A)$ for the SRS (a state of the art system). As a result, $t_\times$ becomes slightly smaller than in fig. 8(a), i.e., the SRS (solid) is preferable to the BIS over a slightly broader range of recovery times in fig. 8(c).

It is possible to increase the value of the response acceleration, A, at which pounding of the BIS occurs by increasing the isolation gap. It is important to note that increasing the isolation gap usually requires additional cost. In fig. 9(a), we assume that the isolation gap is wider than in fig. 5. The loss of functionality of the SRS is the same as in fig. 5. Robustness functions are shown in fig. 9(b). Compared with fig. 8(a), the value of $t_\times$ in fig. 9(b) is larger. Namely, with additional cost of the building, the BIS (dashed) becomes preferable over a broader range of the critical values for the time to recovery. Another issue that one may need to take into account is that, when the response acceleration is very large, it might possibly happen that deformations of the isolators of the BIS exceed the assumed values. If this is the case, the isolators undergo plastic deformations, and the loss of functionality might possibly increase for this reason. Therefore, increase of the isolation gap does not necessarily simply increase of robustness of the BIS. For simplicity, the discussion above

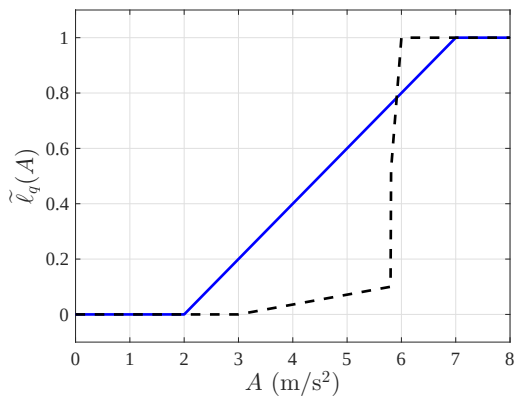

(a)

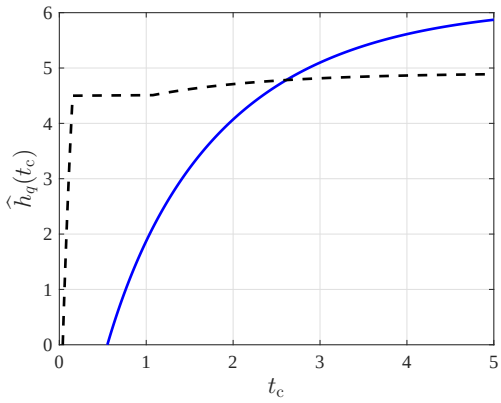

(b)

Figure 9: Robustness analysis for the example in section 3 with larger isolation gap. (a) Estimated loss-of-functionality functions; (b) robustness curves with $(w_{\ell,0}, w_{\ell,1}, w_t) = (0.02, 0.02, 0.05)$. SRS (solid); BIS (dashed).

is restricted to the case in which deformations of the isolators do not exceed the allowable amount.

4 Preference Reversal with Inherent and Exogenous Uncertainty

We now explore a generalization of the example in section 3 with inherent and exogenous uncertainty. We prove a proposition asserting conditions under which the robustness curves for two different designs will cross one another. This crossing of robustness curves entails the potential for reversal of preference between the two designs. Reversal of preference is the basis for the distinction between info-gap robust satisficing and both prediction-based performance optimization and min-max.

We discussed the design and decision implications of crossing robustness curves in connection with figs. 8 and 9. In particular, we explained that the robust preference of one design (e.g. BIS) over another (e.g. SRS) depends on the performance requirement. The info-gap robust satisficing methodology leads the designer to choose the option that is more robust against uncertainty, for achieving a specified performance requirement. Consequently, when the robustness curves for two design alternatives cross one another, the preference between them depends on the performance requirement. The resulting design decision may differ from both the outcome-optimization and the min-max decisions, as discussed in section 2.2. The proposition in this section demonstrates a degree of prevalence and generality of this phenomenon of preference reversal.

Consider two alternative system designs, denoted by $q = 0$ and $q = 1$, where these could for example denote the SRS and BIS designs, respectively. The estimated response acceleration, loss-of-functionality (LOF) function, and time to recovery (TTR) function are $\widetilde{A}$, $\widetilde{\ell}_q(A)$ and $\widetilde{t}(\ell)$, respectively. Uncertainty in these functions is represented by the info-gap models of eqs.(14), (15) and (17). We do not assume the estimated functional form in eq.(16). However, we do assume that the uncertainty weights in the info-gap model of eq.(15) obey:

$$w_{\ell,1} \geq w_{\ell,0} \tag{25}$$

which implies greater uncertainty for functions ℓ_1 than for functions ℓ_0.

We assume that the estimated TTR and LOF functions obey the following relations for all re-

sponse accelerations $A \geq 0$ and for both q values. A_s is a specific value exceeding $\widetilde{A}$:

$$\widetilde{\ell}_1(\widetilde{A}) \;<\; \widetilde{\ell}_0(\widetilde{A}) \tag{26}$$

$$\widetilde{\ell}_1(A) \;>\; \widetilde{\ell}_0(A) \quad \text{if} \quad A_\mathrm{s} \leq A \tag{27}$$

$$\widetilde{\ell}_q(A) \;<\; \widetilde{\ell}_q(A') \quad \text{if} \quad A < A' \tag{28}$$

$$\widetilde{t}(\ell) \;<\; \widetilde{t}(\ell') \quad \text{if} \quad \ell < \ell' \tag{29}$$

Eq.(26) states that the estimated LOF, at the estimated response acceleration, is lower for system 1 than for system 0. In contrast, eq.(27) states that the estimated LOF for system 1 is greater than for system 0 at large accelerations. In other words, eq.(26) states that system 1 is predicted to be less vulnerable than system 0 at the estimated load, but eq.(27) states that system 1 is more vulnerable at large loads. That is, these equations express different vulnerabilities of these two systems. Eqs.(26) and (27) describe the curves in fig. 5. Eq.(28) asserts that estimated LOF functions are monotonically increasing. Eq.(29) asserts that the estimated TTR functions are monotonic, reflecting the situation in fig. 6.

Note that we have not assumed that the actual LOF or TTR functions ℓ_q or t (as distinct from the estimated functions $\widetilde{\ell}_q$ or $\widetilde{t}$) are monotonic. This is a physically reasonable assumption but we do not need it in order to prove proposition 1.

The performance requirement is that the TTR does not exceed a critical value:

$$t(\ell_q(A)) \leq t_\mathrm{c} \tag{30}$$

The robustness function, $\widehat{h}_q(t_\mathrm{c})$, is defined in eq.(18).

We can now assert the following proposition. The proof appears in Appendix B.

Proposition 1 Given:

• The estimated TTR and LOF functions, $\widetilde{t}(\ell)$ and $\widetilde{\ell}_q(A)$, obey the conditions of eqs.(26)–(29).

• The info-gap models, $\mathcal{A}(h)$, $\mathcal{L}_q(h)$ and $\mathcal{T}(h)$, are specified in eqs.(14), (15) and (17) with the further condition of eq.(25).

• The performance requirement is eq.(30).

Then: The robustness curves, defined in eq.(18), intersect one another. $\widehat{h}_1(t_\mathrm{c})$ exceeds $\widehat{h}_0(t_\mathrm{c})$ for a low range of t_c values. $\widehat{h}_0(t_\mathrm{c})$ equals or exceeds $\widehat{h}_1(t_\mathrm{c})$ at higher values of t_c.

This proposition asserts that systems, with the stated vulnerabilities, display different robustness to uncertainties (both inherent and exogenous). Specifically, the vulnerabilities and uncertainties result in crossing robustness curves, and this causes the potential for reversal of preference between the two designs.

5 Summary and Conclusion

All structures have various vulnerabilities to adverse events. However, evaluation of the seismic resilience of structures inevitably encounters severe uncertainties. In particular, the time to recovery of damaged buildings has both endogenous uncertainties (relating to the structure and its subsystems) and exogenous uncertainties (relating to the loads and the surroundings). It is difficult to predict seismic responses of the structure and of nonstructural components, such as the equipment and facilities of buildings, damage of which affect the recovery time. Moreover, it is impossible to

predict the seismic event reliably; natural hazards have repeatedly surprised us with events significantly more severe than historical precedents. Such uncertainty may prevent existing methods for evaluation of the seismic resilience of structures from providing reliable results. A remedy is to incorporate the concept of robustness against such uncertainty into the evaluation method of the resilience.

This paper has presented a framework—info-gap robust satisficing—for evaluation of resilience of a structural system for fully addressing such great uncertainty. The examples in sections 2 and 3 illustrate the robustness analysis. It is noteworthy that the proposed framework does not require reliable predictions of the time to recover, the seismic responses of the structures and the non-structural components, the seismic event, etc. Rather, it is based on the premise that they cannot be predicted precisely. Then, the method ranks alternative structural designs in terms of their robustness against uncertainty for satisficing the requirement of resilient performance. To clarify the generic methodology, in this paper we have consider two examples of the seismic design concepts (i.e., the seismic resistant structure and the base-isolated structure) and have demonstrated how the proposed framework is used to compare the two structures. The proposed framework is generic and is applicable to any structural designs.

The proposition in section 4 establishes that, if the estimated models of two structural systems satisfy certain conditions, then the robust preference between the designs reverses as the performance requirement changes. The assumptions made in this proposition are rather mild. Hence, when choosing between two structural systems, we encounter reversal of the robust preference quite often, particularly when one of the systems is innovative and the other is classical. The proposed robustness analysis method can numerically find the level of the performance requirement at which such reversal of the robust preference occurs, and hence can assist a structural engineer to make reliable design decision.

A Appendix: Derivation of Robustness Curves for the Example in Section 2.2

Let $m_q(h)$ denote the inner maximum in the definition of the robustness, $\widehat{h}_q(t_c)$ in eq.(7). That is, $m_q(h) = \max\{t_q(\alpha) : \alpha \in \mathcal{U}(h)\}$. We see that $m_q(h)$ increases monotonically as h increases, because the uncertainty sets $\mathcal{U}(h)$ in eq.(6) become more inclusive as h increases. The robustness is the greatest h at which $m_q(h) \le t_c$. The monotonicity of $m_q(h)$ implies that the robustness, $\widehat{h}_q(t_c)$, is the greatest value of h at which $m_q(h) = t_c$. In other words, $m_q(h)$ is the inverse of the robustness function:

$$m_q(h) = t_c \quad \text{if and only if} \quad \widehat{h}_q(t_c) = h \tag{31}$$

This means that a plot of h vs. $m_q(h)$ is identical to a plot of $\widehat{h}_q(t_c)$ vs. t_c. We only need to evaluate the functions $m_q(h)$.

For both designs, $m_q(h)$ occurs when the load is maximal: $a = \widetilde{a} + sh$. For the SRS design, t_0 has been defined in eq.(3), and we find:

$$m_0(h) = \alpha_0(\widetilde{a} + sh - \beta_0) \tag{32}$$

For the BIS design, t_0 has been defined in eq.(2), and we find:

$$m_1(h) = \begin{cases} \alpha_1(\widetilde{a} + sh - \beta_1) & \text{if } \widetilde{a} + sh < \delta_1 \;\leftrightarrow\; h < \frac{\delta_1 - \widetilde{a}}{s} \\ \gamma_1(\widetilde{a} + sh - \delta_1) + \alpha_1(\delta_1 - \beta_1) & \text{else} \end{cases} \tag{33}$$

These inverse robustness functions are plotted in fig. 2 by plotting h on the vertical axis and $m_q(h)$ on the horizontal axis.

B Appendix: Proof of Proposition 1

Let $m_q(h)$ denote the inner maximum in the definition of the robustness, eq.(18). The uncertainty sets, $\mathcal{A}(h)$, $\mathcal{L}_q(h)$ and $\mathcal{T}(h)$, become more inclusive as the horizon of uncertainty, h, increases. This implies that $m_q(h)$, defined as the maximum on these sets, is a monotonically increasing function of h. From this we conclude that $m_q(h)$ is the inverse of the robustness function, $\widehat{h}_q(t_\mathrm{c})$. That is:

$$m_q(h) = t_\mathrm{c} \quad \text{if and only if} \quad \widehat{h}_q(t_\mathrm{c}) = h \tag{34}$$

This means that $m_q(h)$ contains all the information that $\widehat{h}_q(t_\mathrm{c})$ contains. In other words, a plot of h vs. $m_q(h)$ is identical to a plot of $\widehat{h}_q(t_\mathrm{c})$ vs. t_c.

Furthermore, from the discussion leading up to eq.(24), we conclude that:

$$m_q(h) = t_q^\star(h) \tag{35}$$

where $t_q^\star(h)$ has been defined in eq.(21). In other words, eq.(35) is an explicit expression for the inverse of the robustness function for each design. We must show that the functions $m_0(h)$ and $m_1(h)$ intersect one another.

First of all, from eqs.(22)–(24):

$$t_q^\star(0) = \widetilde{t}(\widetilde{\ell}_q(\widetilde{A})) \tag{36}$$

Also, eqs.(26) and (29) imply:

$$\widetilde{t}(\widetilde{\ell}_1(\widetilde{A})) < \widetilde{t}(\widetilde{\ell}_0(\widetilde{A})) \tag{37}$$

Combining eqs.(35)–(37) we conclude:

$$m_1(0) < m_0(0) \tag{38}$$

Because $m_q(h)$ is the inverse of $\widehat{h}_q(t_\mathrm{c})$, this relation implies that the robustness curve for design 1, $\widehat{h}_1(t_\mathrm{c})$, sprouts off of the horizontal t_c axis at a lower value than the robustness curve for design 0. Thus $\widehat{h}_1(t_\mathrm{c})$ exceeds $\widehat{h}_0(t_\mathrm{c})$ at low values of t_c.

Now consider large values of h. We must show that there is a value of h for which $m_1(h)$ reaches or exceeds $m_0(h)$.

Referring to the value of A_s in eq.(27), define h_s from:

$$\widetilde{A} + w_A h_\mathrm{s} = A_\mathrm{s} \tag{39}$$

$h_\mathrm{s} > 0$ because $A_\mathrm{s} > \widetilde{A}$ and $w_A > 0$. Eq.(27) implies, for any $h \geq h_\mathrm{s}$:

$$\widetilde{\ell}_1(\widetilde{A} + w_A h) > \widetilde{\ell}_0(\widetilde{A} + w_A h) \tag{40}$$

Thus eq.(25) implies, for any $h \geq h_\mathrm{s}$:

$$(1 + w_{\ell,1} h)\widetilde{\ell}_1(\widetilde{A} + w_A h) > (1 + w_{\ell,0} h)\widetilde{\ell}_0(\widetilde{A} + w_A h) \tag{41}$$

If either of these expressions exceed 1, then it is truncated to the value of 1 by the info-gap model, as stated in eq.(23). We must consider 2 cases.

Case 1. Suppose that the righthand term in eq.(41) is less than 1 for some $h \geq h_{\rm s}$. In this case eqs.(29) and (41) imply

$$\underbrace{(1+w_t h)\widetilde{t}\left[\min\left\{1,\ (1+w_{\ell,1}h)\widetilde{\ell}_1(\widetilde{A}+w_A h)\right\}\right]}_{t_1^\star(h)} > \underbrace{(1+w_t h)\widetilde{t}\left[(1+w_{\ell,0}h)\widetilde{\ell}_0(\widetilde{A}+w_A h)\right]}_{t_0^\star(h)} \tag{42}$$

where the identification of the left and righthand terms as $t_1^\star(h)$ and $t_0^\star(h)$, respectively, results from eq.(24). Thus, eqs.(35) and (42) imply, for this value of h:

$$m_1(h) > m_0(h) \tag{43}$$

Case 2. Now suppose that the righthand term in eq.(41) equals or exceeds 1 for all $h \geq h_{\rm s}$, in which case both terms in eq.(41) equal or exceed 1. In this case both functions are truncated at the value 1 and eq.(42) is an equality and we obtain, for all $h \geq h_{\rm s}$:

$$m_1(h) = (1+w_t h)\widetilde{t}(1) = m_0(h) \tag{44}$$

Recall that $m_q(h)$ is the inverse of the robustness function $\widehat{h}_q(t_{\rm c})$. Thus eqs.(38) and either (43) or (44) imply that the robustness curves of the two designs have intersected one another. ∎

We note, in eq.(43) of Case 1 of this proof, that the inverse robustness curves actually cross one another. In Case 2, in contrast, the upper bound on the LOF functions in the info-gap model of eq.(15) can cause the intersection of the inverse robustness functions, $m_q(h)$, to occur at the point at which they become equal, eq.(44). In this case the robustness functions intersect but do not ever cross one another. If this trucation constraint were removed, then the robustness functions would strictly cross one another.

Acknowledgments

The work of the first author is partially supported by JSPS KAKENHI 26420545 and 17K06633.

References

[1] V. K. Agarwal, J. M. Niedzwecki, J. W. van de Lindt: Earthquake induced pounding in friction varying base isolated buildings. *Engineering Structures*, **29**, 2825–2832 (2007).

[2] Y. Ben-Haim: *Info-Gap Decision Theory: Decisions under Severe Uncertainty* (2nd ed.). Academic Press, London (2006).

[3] P. Bocchini, D. M. Frangopol: Optimal resilience- and cost-based postdisaster intervention prioritization for bridges along a highway segment. *Journal of Bridge Engineering (ASCE)*, **17**, 117–129 (2012).

[4] P. Bocchini, D. M. Frangopol, T. Ummenhofer, T. Zinke: Resilience and sustainability of civil infrastructure: toward a unified approach. *Journal of Infrastructure Systems (ASCE)*, **20**, 04014004 (2014).

[5] N. Brooks: Vulnerability, risk and adaptation: a conceptual framework. Tyndall Centre for Climate Change Research Working Paper 38, September 2003.

[6] M. Bruneau, S. E. Chang, R. T. Eguchi, G. C. Lee, T. D. O'Rourke, A. M. Reinhorn, M. Shinozuka, K. Tierney, W. A. Wallace, D. von Winterfeldt: A framework to quantitatively assess and enhance the seismic resilience of communities. *Earthquake Spectra*, **19**, 733–752 (2003).

[7] M. Bruneau, A. Reinhorn: Exploring the concept of seismic resilience for acute care facilities. *Earthquake Spectra*, **23**, 41–62 (2007).

[8] Z. Çağnan, R. A. Davidson, S. D. Guikema: Post-earthquake restoration planning for Los Angeles electric power. *Earthquake Spectra*, **22**, 589–608 (2006).

[9] S. Chandrasekaran, S. Banerjee: Retrofit optimization for resilience enhancement of bridges under multihazard scenario. *Journal of Structural Engineering (ASCE)*, C4015012 (2015).

[10] S. E. Chang, M. Shinozuka: Measuring improvements in the disaster resilience of communities. *Earthquake Spectra*, **20**, 739–755 (2004).

[11] A. C. Chopra: *Dynamics of Structures: Theory and Applications to Earthquake Engineering (4th ed.)*. Prentice Hall, Upper Saddle River (2012).

[12] G. P. Cimellaro, M. Malavisi, S. Mahin: Using discrete event simulation models to evaluate resilience of an emergency department. *Journal of Earthquake Engineering*, **21**, 203–226 (2017).

[13] G. P. Cimellaro, A. M. Reinhorn, M. Bruneau: Framework for analytical quantification of disaster resilience. *Engineering Structures*, **32**, 3639–3649 (2010).

[14] G. P. Cimellaro, A. R. Reinhorn, M. Bruneau: Seismic resilience of a hospital system. *Structure and Infrastructure Engineering*, **6**, 127–144 (2010).

[15] G. P. Cimellaro, A. R. Reinhorn, M. Bruneau: Performance-based metamodel for healthcare facilities. *Earthquake Engineering and Structural Dynamics*, **40**, 1197–1217 (2011).

[16] G. Cimellaro, C. Renschler, A. M. Reinhorn, L. Arendt: PEOPLES: a framework for evaluating resilience. *Journal of Structural Engineering (ASCE)*, 04016063 (2016).

[17] G. P. Cimellaro, D. Solari, M. Bruneau: Physical infrastructure interdependency and regional resilience index after the 2011 Tohoku Earthquake in Japan. *Earthquake Engineering and Structural Dynamics*, **43**, 1763–1784 (2014).

[18] G. P. Cimellaro, A. Tinebra, C. Renschler, M. Fragiadakis: New resilience index for urban water distribution networks. *Journal of Structural Engineering (ASCE)*, **142**, C4015014 (2016).

[19] G. P. Cimellaro, A. Tinebra, C. Renschler, M. Fragiadakis: Closure to "New Resilience Index for Urban Water Distribution Networks" by G. P. Cimellaro, A. Tinebra, C. Renschler, and M. Fragiadakis. *Journal of Structural Engineering (ASCE)*, to appear. DOI:10.1061/(ASCE)ST.1943-541X.0001813.

[20] Y. Dong, D. M. Frangopol: Risk and resilience assessment of bridges under mainshock and aftershocks incorporating uncertainties. *Engineering Structures*, **83**, 198–208 (2015).

[21] Y. Dong, D. M. Frangopol: Performance-based seismic assessment of conventional and base-isolated steel buildings including environmental impact and resilience. *Earthquake Engineering and Structural Dynamics*, **45**, 739–756 (2016).

[22] J. F. Hall, T. H. Heaton, M. W. Halling, D. J. Wald: Near-source ground motion and its effects on flexible buildings. *Earthquake Spectra*, **11**, 569–605 (1995).

[23] P. Komodromos: Simulation of the earthquake-induced pounding of seismically isolated buildings. *Computers and Structures*, **86**, 618–626 (2008).

[24] P. Komodromos, P. C. Polycarpou, L. Papaloizou, M. C. Phocas: Response of seismically isolated buildings considering poundings. *Earthquake Engineering and Structural Dynamics*, **36**, 1605–1622 (2007).

[25] P. K. Malhotra: Dynamics of seismic impacts in base-isolated buildings. *Earthquake Engineering and Structural Dynamics*, **26**, 797–813 (1997).

[26] A. Masroor, G. Mosqueda: Experimental simulation of base-isolated buildings pounding against moat wall and effects on superstructure response. *Earthquake Engineering and Structural Dynamics*, **41**, 2093–2109 (2012).

[27] A. Masroor, G. Mosqueda: Impact model for simulation of base isolated buildings impacting flexible moat walls. *Earthquake Engineering and Structural Dynamics*, **42**, 357–376 (2013).

[28] V. A. Matsagar, R. S. Jangid: Seismic response of base-isolated structures during impact with adjacent structures. *Engineering Structures*, **25**, 1311–1323 (2003).

[29] F. Mazza, A. Vulcano: Effects of near-fault ground motions on the nonlinear dynamic response of base-isolated r.c. framed buildings. *Earthquake Engineering and Structural Dynamics*, **41**, 211–232 (2012).

[30] T. McDaniels, S. Chang, D. Cole, J. Mikawoz, H. Longstaff: Fostering resilience to extreme events within infrastructure systems: characterizing decision contexts for mitigation and adaptation. *Global Environmental Change*, **18**, 310–318 (2008).

[31] J. Mochizuki, N. Komendantova: In search of perfect foresight? Policy bias, management of unknowns, and what has changed in science policy since the Tohoku disaster. *Risk Analysis*, **37**, 219–230 (2017).

[32] S. Nagarajaiah, X. Sun: Base-isolated FCC building: impact response in Northridge earthquake. *Journal of Structural Engineering (ASCE)*, **127**, 1063–1075 (2001).

[33] T. R. Neelakantan, C. R. Suribabu: Discussion of “New Resilience Index for Urban Water Distribution Networks” by G. P. Cimellaro, A. Tinebra, C. Renschler, and M. Fragiadakis. *Journal of Structural Engineering (ASCE)*, **143**, 07017001 (2017).

[34] R. Pant, K. Barker, C. W. Zobel: Static and dynamic metrics of economic resilience for interdependent infrastructure and industry sectors. *Reliability Engineering and System Safety*, **125**, 92–102 (2014).

[35] D. R. Pant, A. C. Wijeyewickrema: Structural performance of a base-isolated reinforced concrete building subjected to seismic pounding. *Earthquake Engineering and Structural Dynamics*, **41**, 1709–1716 (2012).

[36] D. R. Pant, A. C. Wijeyewickrema: Performance of base-isolated reinforced concrete buildings under bidirectional seismic excitation considering pounding with retaining walls including friction effects. *Earthquake Engineering and Structural Dynamics*, **43**, 1521–1541 (2014).

[37] A. G. Pateli: Decision making on governance of strategic technology alliances. *Management Decision*, **47**, 246–270 (2009).

[38] P. C. Polycarpou, P. Komodromos: Earthquake-induced poundings of a seismically isolated building with adjacent structures. *Engineering Structures*, **32**, 1937–1951 (2010).

[39] P. C. Polycarpou, P. Komodromos: On poundings of a seismically isolated building with adjacent structures during strong earthquakes. *Earthquake Engineering and Structural Dynamics*, **39**, 933–940 (2010).

[40] P. C. Polycarpou, P. Komodromos, A. C. Polycarpou: A nonlinear impact model for simulating the use of rubber shock absorbers for mitigating the effects of structural pounding during earthquakes. *Earthquake Engineering and Structural Dynamics*, **42**, 81–100 (2013).

[41] K. A. Porter, A. S. Kiremidjian, J. S. LeGrue: Assembly-based vulnerability of buildings and its use in performance evaluation. *Earthquake Spectra*, **17**, 291–312 (2001).

[42] K. Tierney, M. Bruneau: Conceptualizing and measuring resilience: a key to disaster loss reduction. *TR News*, **250**, 14–17 (2007).

[43] H.-C. Tsai: Dynamic analysis of base-isolated shear beams bumping against stops. *Earthquake Engineering and Structural Dynamics*, **26**, 1096–9845 (1997).

[44] L. Tirca, O. Serban, L. Lin, M. Wang, N. Lin: Improving the seismic resilience of existing braced-frame office buildings. *Journal of Structural Engineering (ASCE)*, C4015003 (2015).

[45] Z. Qu, S. Kishiki, T. Nakazawa: Influence of isolation gap size on the collapse performance of seismically base-isolated buildings. *Earthquake Spectra*, **29**, 1477–1494 (2013).

[46] J. Sharma, R. K. Chaturvedi, G. Bala, N. H. Ravindranath: Assessing “inherent vulnerability” of forests: a methodological approach and a case study from Western Ghats, India. *Mitigation and Adaptation Strategies for Global Change*, **20**, 573–590 (2015).